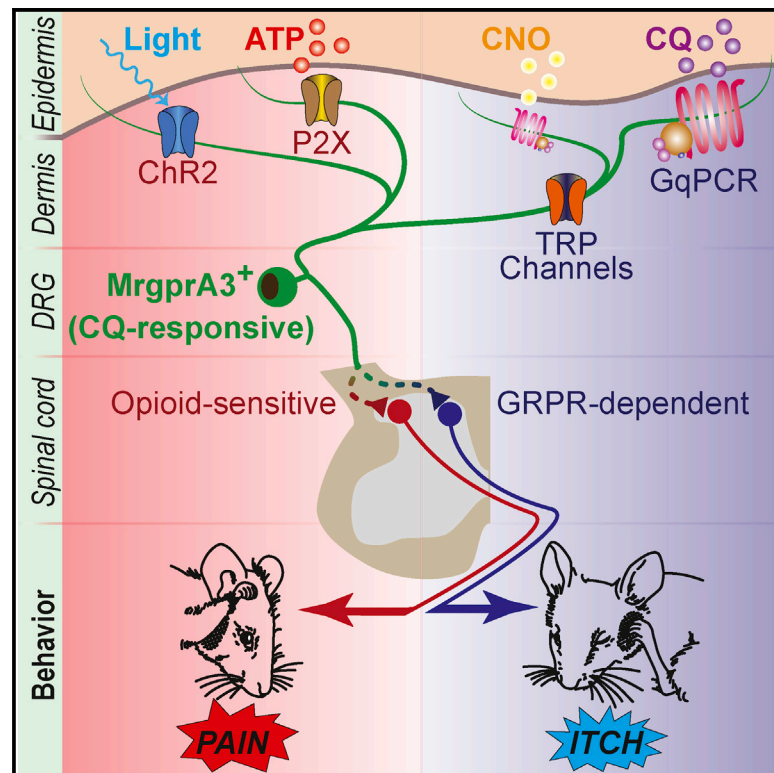


# Neuron

## Differential Coding of Itch and Pain by a Subpopulation of Primary Afferent Neurons

### Graphical Abstract



### Authors

Behrang Sharif, Ariel R. Ase,  
Alfredo Ribeiro-da-Silva,  
Philippe Séguéla

### Correspondence

philippe.seguela@mcgill.ca

### In Brief

Sharif et al. present evidence that a subpopulation of peripheral chloroquine-responsive somatosensory afferents can differentially drive itch or pain responses when they are stimulated via metabotropic or fast ionotropic signaling pathways, respectively.

### Highlights

- Metabotropic Gq-linked stimulation of MrgprA3 C-afferents triggers itch
- Ionotropic stimulation of MrgprA3 C-afferents through ChR2 or native P2X3 evokes pain
- Evoked itch and pain responses differentially engage spinal GRPR and opioid pathways
- Pruriceptive, but not nociceptive, responses are alleviated by blockade of TRP channels

# Differential Coding of Itch and Pain by a Subpopulation of Primary Afferent Neurons

Behrang Sharif<sup>1,2,3</sup>, Ariel R. Ase<sup>1,2</sup>, Alfredo Ribeiro-da-Silva<sup>2,4</sup>, and Philippe Séguéla<sup>1,2,5,\*</sup>

<sup>1</sup>Montreal Neurological Institute, Department of Neurology & Neurosurgery, McGill University, Montreal, QC H3A 2B4, Canada

<sup>2</sup>Alan Edwards Centre for Research on Pain, Montreal, QC H3A 0G1, Canada

<sup>3</sup>Department of Physiology, McGill University, Montreal, QC H3G 1Y6, Canada

<sup>4</sup>Department of Pharmacology & Therapeutics, McGill University, Montreal, QC H3G 1Y6, Canada

<sup>5</sup>Lead Contact

\*Correspondence: [philippe.seguela@mcgill.ca](mailto:philippe.seguela@mcgill.ca)

<https://doi.org/10.1016/j.neuron.2020.03.021>

## SUMMARY

Itch and pain are distinct unpleasant sensations that can be triggered from the same receptive fields in the skin, raising the question of how pruriception and nociception are coded and discriminated. Here, we tested the multimodal capacity of peripheral first-order neurons, focusing on the genetically defined subpopulation of mouse C-fibers that express the chloroquine receptor MrgprA3. Using optogenetics, chemogenetics, and pharmacology, we assessed the behavioral effects of their selective stimulation in a wide variety of conditions. We show that metabotropic Gq-linked stimulation of these C-afferents, through activation of native MrgprA3 receptors or DREADDs, evokes stereotypical pruriceptive rather than nocifensive behaviors. In contrast, fast ionotropic stimulation of these same neurons through light-gated cation channels or native ATP-gated P2X3 channels predominantly evokes nocifensive rather than pruriceptive responses. We conclude that C-afferents display intrinsic multimodality, and we provide evidence that optogenetic and chemogenetic interventions on the same neuronal populations can drive distinct behavioral outputs.

## INTRODUCTION

Itch and pain are the primary presenting symptoms in most clinical visits (St Sauver et al., 2013) and the causes of disability in many burdensome diseases (Vos et al., 2016). Basic understanding of how distinct somatosensory modalities are transduced and perceived in healthy and disease states has significantly improved with the identification of neuronal subcategories and spinal pathways. In particular, primary afferents have been categorized and characterized extensively (Le Pichon and Chesler, 2014; Usoskin et al., 2015; Zeisel et al., 2018). Despite advancements in understanding somatosensory transduction, the basic principles of sensory modality discrimination, especially for overlapping modalities such as itch and pain, remain unclear.

Itch is defined as an unpleasant sensation that leads to scratching or the desire to scratch, a behavior aimed at removal of chemical or mechanical irritants. Similarly, pain can also be described as an unpleasant sensation, with the difference being that it leads to withdrawal or mitigating behavior rather than scratching. Pruriception and nociception share anatomical pathways (Davidson and Giesler, 2010; Klein et al., 2011) and influence one another (Brull et al., 1999; Nilsson et al., 1997; Simone et al., 2004). However, this close relationship, contrasted by distinct behavioral outcomes, poses a conundrum: how does the somatosensory system differentiate itch from pain to trigger the appropriate response, i.e., fight (removal) or flight (withdrawal)?

Historically, various models for somatosensory discrimination have been proposed based on intensity of stimuli, firing pattern of the afferents, subcategories of modality-specific neuronal populations, or spatial pattern of the stimuli (LaMotte et al., 2014; McMahon and Koltzenburg, 1992; Schmelz, 2015). The most-studied model for itch is the “labeled line” or “specificity” theory, which states that dedicated cellular components, from the periphery to the brain, are specialized for pruriceptive transduction, transmission, and perception (McMahon and Koltzenburg, 1992). The Mas1-related G-protein-coupled receptor A3 (MrgprA3)-expressing subpopulation of unmyelinated (C) afferents has been proposed as one labeled line for itch (Han et al., 2013). Mrgprs constitute a family of G-protein-coupled receptors enriched in non-peptidergic primary somatosensory neurons (Dong et al., 2001; Lembo et al., 2002; Liu et al., 2009; Zylka et al., 2003). MrgprA3, or its human ortholog MrgprX1, is the main receptor of the pruritogenic compound chloroquine (CQ), and converging evidence indicates that the MrgprA3-expressing primary sensory neurons specifically mediate CQ-induced itch responses (Han et al., 2013; Liu et al., 2009; Ru et al., 2017). As no significant reduction in pain behavior was observed following ablation of MrgprA3 C-afferents in adult mice, their dispensability for nociception was inferred. Essentiality and sufficiency of these neurons for pruriception were also demonstrated, as their ablation leads to a reduction in itch behavior while their activation by capsaicin in *Trpv1<sup>-/-</sup>;MrgprA3<sup>Cre-EGFP</sup>;ROSA26<sup>Trpv1</sup>* mice resulted predominantly in scratching behaviors (Han et al., 2013).

Other peripheral labeled lines have been characterized as pruriceptive primary afferents, including somatostatin-expressing

neurons responsible for itch induced by I1-31 and 5HT (Stantcheva et al., 2016), MrgprA3<sup>-</sup> histamine-sensitive pruriceptors (Roberson et al., 2013), and MrgprD afferents mediating  $\beta$ -alanine-induced itch (Liu et al., 2012). Tallying the labeled lines for itch results in a large proportion of primary somatosensory neurons including most non-peptidergic C-fibers reported as mechano-nociceptors (Scherrer et al., 2009). The simple fact that these pruriceptors can also respond to noxious stimuli calls for alternative models, as the specificity theory requires the existence of a subset of primary sensory neurons that respond to pruritogenic stimuli and no other (McMahon and Koltzenburg, 1992).

Attesting to intrinsic multimodality of primary sensory neurons, we report here that metabotropic stimulation of MrgprA3 C-afferents predominantly triggers itch while fast ionotropic stimulation of the same neuronal population predominantly drives pain. We further confirm distinct sensory perceptions by pharmacological interference with gastrin-releasing peptide (GRP) signaling for itch or opioid signaling for pain. We also show that, downstream of MrgprA3 C-afferent stimulation, pruriception depends on the recruitment of calcium-permeable transient receptor potential (TRP) channels, whereas these channels do not contribute to nociception, providing a molecular basis for somatosensory discrimination at the peripheral level. Finally, we demonstrate for the first time that the MrgprA3 C-afferents indeed contribute to acute pain coding as their conditional silencing significantly reduces ATP-induced nocifensive responses.

## RESULTS

### Metabotropic Activation of MrgprA3 C-Afferents Induces Itch

CQ induces itch through activation of the G-protein-coupled MrgprA3 receptor. The dependence of CQ-induced pruriception on MrgprA3 has been established by knockout and rescue experiments (Liu et al., 2009). To test the sufficiency of metabotropic receptor activation for the induction of itch, we expressed the excitatory Gq-coupled DREADD hM3Dq-mCherry (Urban and Roth, 2015) in MrgprA3<sup>+</sup> neurons through adeno-associated virus (AAV)-mediated delivery in hemizygote MrgprA3<sup>Cre-EGFP</sup> mice. Viral transduction efficiency and expression of heterologous hM3Dq in dorsal root ganglia (DRGs) were validated by immunofluorescence of mCherry (Figure 1A). The EGFP fused to Cre recombinase in MrgprA3<sup>Cre-EGFP</sup> mice allowed visualization and counting of MrgprA3<sup>+</sup> cells. We observed a relatively small population of MrgprA3<sup>+</sup> C-afferents in the primary sensory ganglia (8.6%  $\pm$  1.3% SEM, 18 DRG sections, 6 animals). A viral transduction efficiency of 44.4%  $\pm$  5.1% (SEM) was observed in Cre-EGFP-expressing neurons with almost perfect specificity (i.e., complete overlap of hM3Dq-mCherry and Cre-EGFP reporter). Functionally, hM3Dq-evoked excitation of virally transduced MrgprA3 neurons was validated by ratiometric calcium imaging using the DREADD agonist clozapine N-oxide (CNO) *in vitro* (Figure 1B). From the 12 recordings performed on primary DRG cultures from 3 animals, 61 EYFP<sup>+</sup> cells were analyzed as they responded to the positive control high KCl. Out of the 61 cells, 50 cells (82%) were responsive to CQ and 12 cells (20%) showed calcium transients in response to CNO. To study the behavioral consequences of *in vivo* activation of MrgprA3 C-af-

ferents through heterologous Gq-coupled receptors, scratching responses to 3 mM CNO injection in the nape of the neck of AAV hM3Dq-mCherry-transduced mice were compared to responses of their MrgprA3<sup>Cre-EGFP<sup>-/-</sup></sup> cage/littermates who also received postnatal AAVs (Figures 1C–1F). Animals were videotaped from three angles (Figure S1A) for 60 min after injection. Accurate and unbiased measurement of each scratching bout was performed offline by a blinded experimenter identifying all start and end points. The number of scratching bouts and sum of durations spent scratching for each individual mouse in every 30-s bin after injection is visualized in separate heatmaps (Figure 1C). To qualitatively study the behaviors, we documented the distribution of durations of individual scratching bouts for every single scratching behavior observed (Figure 1D). This measurement indicates how effective the scratching is, and the similarity of the distribution histograms suggests a similar perceptive state. Our scoring approach also enables us to detect changes in behavior over time (Figure 1E) as well as overall differences over the 1-h period (Figure 1F). CNO injection in the nape of the neck of AAV-injected Cre<sup>-</sup> mice did not induce scratching (Figure 1C), whereas in their Cre<sup>+</sup> cagemate littermates, a robust itch developed soon after injection (Figure 1E), resulting in significantly higher total number of bouts (Figure 1F). When the same Cre<sup>+</sup> animals received 10 mM CQ (Green et al., 2006), pruritus built up for a longer period of time (Figure 1E) with higher intensity (Figures 1E and 1F) compared to the itch induced by CNO. Comparable bout durations resulted in a similar, and statistically akin, time course and total time of scratching (Figures S1B and S1C).

In agreement with previous reports (Han et al., 2013), our results indicate that selective chemical stimulation of MrgprA3 C-afferents induces pruriception. The intensity of itch responses caused by the activation of endogenous MrgprA3 receptors by CQ was significantly higher than the intensity of itch responses evoked by selective stimulation of the DREADD-expressing subset. The weaker response may be attributed to viral transduction (i.e., smaller afferent population activated), different levels of expression of hM3Dq and MrgprA3 receptors at the surface of the afferents, suboptimal coupling of the DREADD to intracellular signaling pathways, or the different pharmacokinetic properties of the agonists CNO and CQ.

### Selective Light-Gated Ionotropic Activation of MrgprA3 C-Afferents Induces Aversive Responses Distinct from Scratching

To test a different mode of stimulation on the same genetically defined primary afferents, we expressed the excitatory light-gated actuator channelrhodopsin-2 (ChR2) in MrgprA3<sup>+</sup> neurons by crossing transgenic lines to produce MrgprA3<sup>Cre-EGFP<sup>+/-</sup></sup>; Rosa26<sup>ChR2-EYFP<sup>+/-</sup></sup> animals. Selective Cre-dependent expression of ChR2 in MrgprA3<sup>+</sup> neurons was validated by the localization of their respective conjugated fluorophores, membrane-bound EYFP for ChR2 and nuclear EGFP for Cre (Figure S2A), in primary sensory ganglia (Figure 2A). Trafficking of ChR2 to peripheral terminals was validated by the EYFP signal observed in the epidermis of the nape of the neck counterstained with the peripheral neural marker PGP9.5 (Figure 2B), confirming the feasibility of transdermal illumination for activation of cutaneous MrgprA3<sup>+</sup> nerve endings. In order to check the functionality of

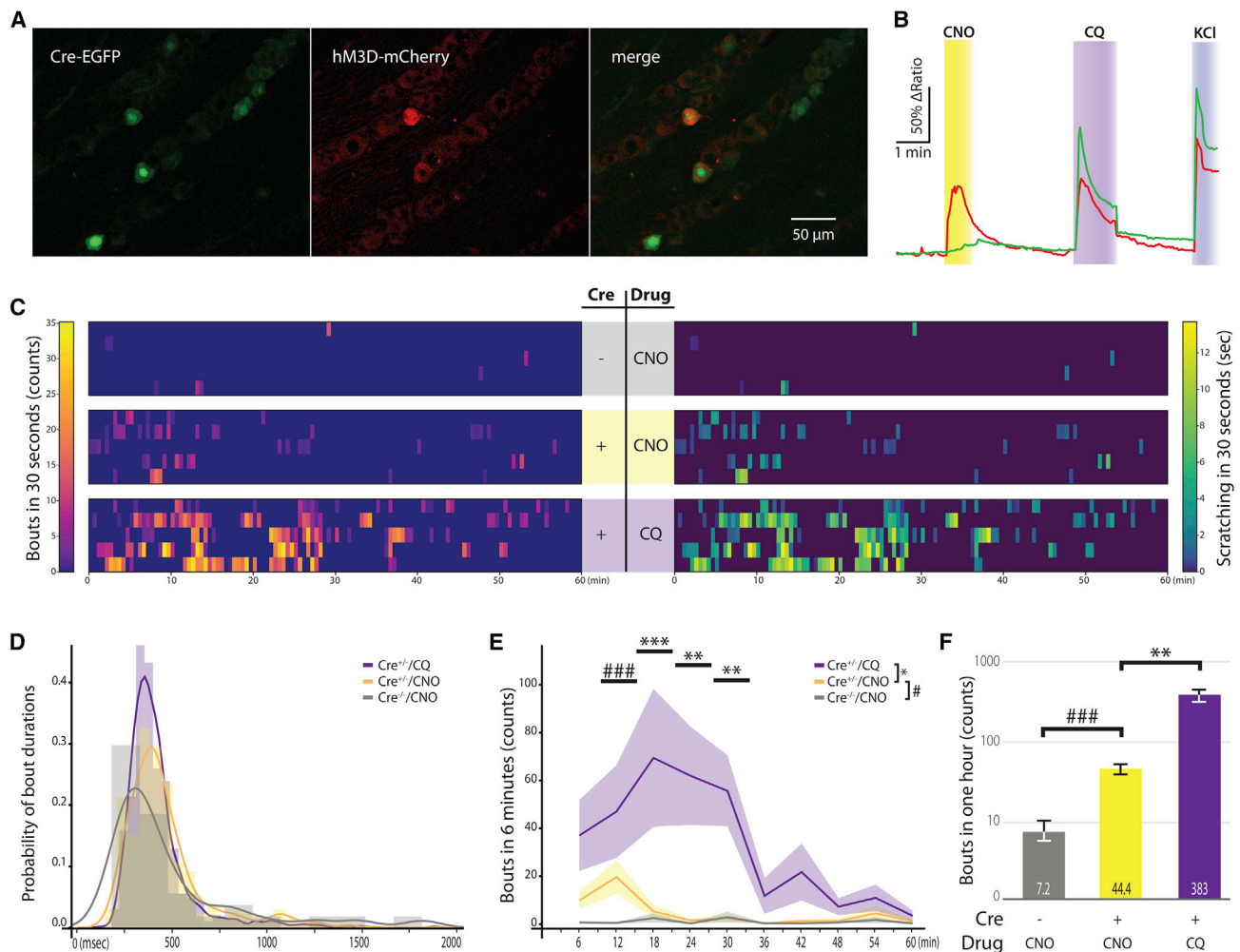


**Figure 1. Selective Stimulation of MrgprA3 C-Afferents via Activation of Endogenous or Heterologous Metabotropic Receptors Induces Scratching**

(A) AAV transduction induces selective Cre-dependent expression of hM3Dq-mCherry in MrgprA3<sup>Cre-EGFP</sup> cells. The Cre-EGFP signal is predominantly localized in the nucleus; the mCherry signal was amplified with a monoclonal antibody against mCherry.

(B) Calcium transients evoked by CNO (5  $\mu$ M) or CQ (2 mM) validate the selective activation of MrgprA3 neurons *in vitro*. Representative traces from a Cre-EGFP<sup>+</sup>:mCherry<sup>-</sup> cell (green trace) and a Cre-EGFP<sup>+</sup>:mCherry<sup>+</sup> cell (red trace). KCI (50 mM) was used as positive control.

(C) CNO (3 mM) induces a hM3Dq-mediated scratching behavior that is similar to, but not as intense as, that induced by CQ (10 mM). Shown is the time course of scratching behavior induced by intradermal injection of CNO in Cre<sup>-/-</sup> animals (top), CNO in Cre<sup>+/-</sup> cagemates/littermates (middle), and CQ in the same Cre<sup>+/-</sup> animals (bottom). Each row in every panel represents an individual mouse (n = 5 for each condition). Compounds were injected at time = 0, and every colored block indicates the number of scratching bouts (left) or the time spent scratching (right) in the corresponding 30-s bin, as defined by the color maps. Rare sporadic baseline scratching behavior in Cre<sup>-/-</sup>/CNO group shows a different profile compared to that of Cre<sup>+/-</sup>/CNO and Cre<sup>+/-</sup>/CQ groups that display significant responses closer to injection time.

(D) Probability distributions of scratching bout durations show that although total counts are different (36, 222, and 1,946 for the Cre<sup>-/-</sup>/CNO, Cre<sup>+/-</sup>/CNO, and Cre<sup>+/-</sup>/CQ groups, respectively), mean durations of individual bouts are similar (495.4, 471.9, and 429.5 ms for the Cre<sup>-/-</sup>/CNO, Cre<sup>+/-</sup>/CNO, and Cre<sup>+/-</sup>/CQ groups, respectively).

(E) Native MrgprA3 or Gq-coupled DREADD activation induces comparable buildup and wind down of scratching behavior over time, albeit with different intensities. Timeline of scratching bout counts indicates that unlike Cre<sup>-/-</sup>/CNO group, metabotropic activation in the Cre<sup>+/-</sup>/CNO and Cre<sup>+/-</sup>/CQ groups induces scratching behavior closer to injection time. While CNO induces significantly more scratching bouts in Cre<sup>+/-</sup> than in Cre<sup>-/-</sup> animals, CQ effects in the same Cre<sup>+/-</sup> animals last longer and build up to a higher extent. Two-way ANOVA and Bonferroni post hoc tests were used for comparison of Cre (#) or drug effects (\*) over time. The 1-h period of observation (compound injection at time = 0) was divided into 10 equal 6-min bins in order to perform the statistical tests.

(F) CNO induces itch only in presence of hM3Dq and in lower intensities than CQ. Total numbers of scratching bouts over the 1-h period following CNO injection show significant scratching behavior in Cre<sup>+/-</sup> and Cre<sup>-/-</sup> animals (unpaired t test, p < 0.001). The itch behavior induced by CQ is significantly more intense than the one induced by CNO (paired t test, p < 0.01).

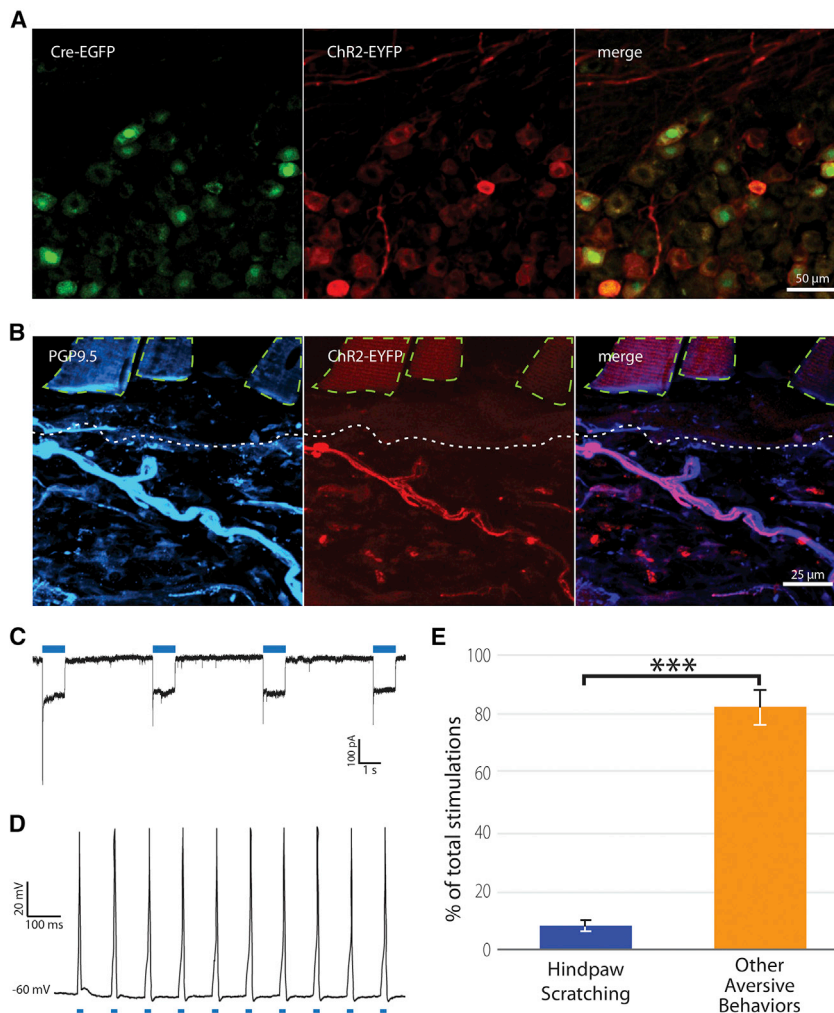


**Figure 2. Optical Ionotropic Stimulation of ChR2-Expressing MrgprA3 C-Afferents Mainly Induces Aversive Behaviors other than Scratching**

(A)  $MrgprA3^{Cre-EGFP+/-};Rosa26^{ChR2-EYFP+/-}$  animals express channelrhodopsin-2 (ChR2) in  $MrgprA3^+$  primary afferents in cervical dorsal root ganglia. Representative image shows nuclear Cre-EGFP, while the EYFP signal in the same neurons shows the expression of ChR2 on the cell membrane and in processes (Figure S2A).

(B) ChR2 is trafficked to the peripheral terminals in the skin of the nape of the neck. ChR2-EYFP is detected in peripheral nerve endings (stained by PGP9.5) in the hairy skin. Hair shafts are indicated by dashed lines, and the dermis-epidermis border is indicated by a dotted line.

(C) ChR2 photocurrents evoked by blue light in response to four 1-s-long stimulations in voltage clamp.

(D) Generation of a train of action potentials by 20-ms short pulses of blue light confirms the capability of these cells to follow frequencies up to 10 Hz reliably.

(E) *In vivo* photostimulation of the nape of the neck induces behavioral responses in most trials ( $89.9\% \pm 0.05\%$  SEM of all stimulations, 6 animals, 15 stimulations each). A majority of these responses correspond to aversive behaviors such as escaping, aggressive approaches, or vocalization (other aversive behaviors) instead of stereotypical itch behaviors (rapid scratching bouts with the hindpaws) ( $p < 0.001$ ).

the excitatory opsins in  $MrgprA3^+$  neurons, *in vitro* electrophysiology experiments were performed. Recordings on ChR2<sup>+</sup> cells confirmed inward photocurrents ( $7.54 \pm 1.24$  pA/pF, 20 cells, 3 animals) (Figure 2C), optically induced action potentials, and firing frequencies of up to 10 Hz driven by blue (470-nm) laser pulses (Figure 2D). Blue laser illumination of the nape of the neck evoked behavioral responses distinct from stereotypical scratching behavior. Other aversive behaviors such as vocalization, escaping, and attempts to bite the light source, rather than scratching, constituted the vast majority of responses evoked by transdermal optical stimulation (Figure 2E; Video S1). We did not observe a correlation between the frequency or intensity of the laser pulses and the type of elicited behavior despite screening multiple protocols of frequency-intensity combinations. Similar illumination of control  $MrgprA3^{Cre-EGFP-/-};Rosa26^{ChR2-EYFP+/-}$  cagemate littermates did not elicit any behavioral responses above background (Video S2), nor did yellow (589-nm) laser pulses with same or higher intensity in the same animals, indicating that the responses are generated through ChR2 channels rather than through thermal or visual effects of light pulses.

These results demonstrate that similar to other subsets of primary somatosensory neurons (Daou et al., 2013),  $MrgprA3$  C-afferents can be controlled *in vitro* and *in vivo* by optogenetic actuators. They also suggest that nocifensive responses are evoked by optical stimulations of  $MrgprA3$  C-afferents, although in rare occasions, stereotypical pruriceptive behaviors can be observed.

### MrgprA3 C-Afferents Trigger Distinct Somatosensory Perceptions Based on Their Activation Mode

In order to clarify the sensory modalities evoked by differential activation of  $MrgprA3$ -expressing fibers, we used the cheek behavioral discrimination assay (Shimada and LaMotte, 2008). Although the nape assay represents a common behavioral assay for studying itch in mice, it cannot definitively discriminate between itch and pain. In the cheek assay, however, pruritogenic stimuli evoke hindpaw scratching while algogenic stimuli evoke unilateral forepaw wiping (Shimada and LaMotte, 2008). Therefore, to confirm the sensory modality perceived following excitatory DREADD activation, AAV-injected  $MrgprA3^{Cre-EGFP+/-}$  animals were videotaped from different angles for 1 h after injection of CNO in the cheek. Accurate frame-by-frame timings of scratching bouts and unilateral wipes targeted to the site of administration, i.e., ipsilateral to the injection, were recorded offline by a blinded experimenter (Video S3). The timeline of both behaviors in each individual mouse is

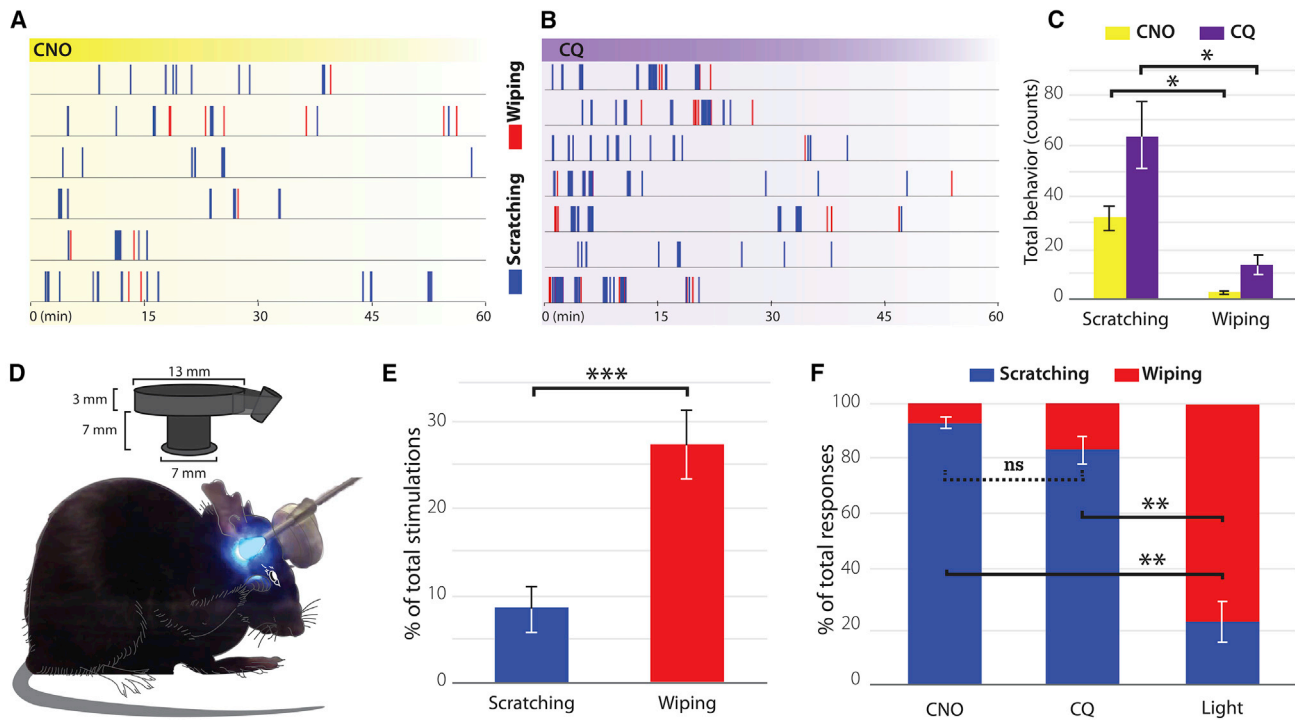


**Figure 3. Distinct Stimulation Modes of Cutaneous MrgprA3 C-Afferents Differentially Evoke Itch or Pain with Stereotypical Behavioral Responses**

(A and B) Time course of pruriceptive hindpaw scratching bouts (blue) and nocifensive forepaw wipes (red) following injection of (A) CNO (3 mM) and (B) CQ (10 mM) in the cheek. Each row represents an individual animal ( $n = 6-7$ ), and each behavioral event is represented by colored bars at the corresponding time. (C) Compilation of behavioral responses ( $p < 0.05$ ). (D) 3D-printed headposts (top) as fiber optic holders for consistent cheek illumination. Transdermal blue laser illumination on the cheek induces stereotypical nocifensive wiping behavior (bottom, Video S4). (E) Probability of light-induced wiping and scratching (5 animals, 15 test sessions, 8 trials each,  $p < 0.001$ ). (F) Behavioral phenotype in metabotropic (i.e., CNO and CQ) versus ionotropic (i.e., blue light) stimulation ( $p < 0.01$  for both, one-way ANOVA with Bonferroni post hoc test).

shown in Figure 3A. Similarly, behavioral responses evoked by activation of MrgprA3 by CQ in the cheek of wild-type mice were analyzed (Figure 3B). In both conditions, animals exhibited significantly higher counts of scratching bouts than wipings (Figure 3C), indicating pruriception. Similar to our results in the neck (Figure 2), the scratching induced by CQ is stronger than that of CNO (Figure S2B). To be able to unambiguously assess the sensory modality associated with optical activation of MrgprA3-expressing fibers, we designed an optogenetic version of the cheek assay after confirmation of ChR2 expression in trigeminal ganglia and trafficking to the cheek hairy skin (Figures S2C and S2D). In order to keep constant both location and light power for transdermal optical stimulation of the cheek with a blue laser, and also to avoid movement hindering, custom 3D-printed headposts were designed as optical fiber holders (Figure 3D). Headposts were chronically implanted on the skull of adult MrgprA3<sup>Cre-EGFP+/-</sup>; Rosa26<sup>ChR2-EYFP+/-</sup> mice several weeks before the experiments (Figure 3D). Acclimated animals then received 470-nm blue laser pulses on their cheek, and the behavioral responses (i.e., forepaw wiping or hindpaw scratching) were recorded. Restricting the illumination site to the same single spot on the skin increased the probability of desensitization after a few stimulations. To minimize desensitization, each animal received a maximum of 8 trains of

light pulses (trials) in each experiment session, and the sessions were at least 48 h apart. With this approach, light-evoked behavioral responses were observed in  $36.25\% \pm 3.9\%$  (SEM) of the trials (5 animals, 15 sessions total, with 8 trials per session). Stereotypical pain-associated cheek wipings were observed in most responses ( $77.6\% \pm 7.0\%$  SEM) to blue light pulses (Figure 3E; Video S4). The same animals did not respond to yellow light pulses with similar or higher laser power in control experiments (Video S5), confirming that the behavioral responses are induced by ionotropic excitation of MrgprA3 C-afferents through ChR2 activation. Furthermore, the control MrgprA3<sup>Cre-EGFP+/-</sup>; Rosa26<sup>ChR2-EYFP+/-</sup> cagemate littermates showed no response to similar illumination, ruling out the effect of bright light causing aversion and/or visual distraction (Video S6). The perception evoked by fast ionotropic activation of these MrgprA3 C-afferents is distinct from the perception evoked by their metabotropic activation, and this multimodality is supported by distinct wiping/scratching ratios in the cheek assay (Figure 3F).

Our results demonstrate that the MrgprA3 C-afferents are intrinsically capable of multimodal sensory coding based on their activation mode. For the first time, we provide evidence that a single population of primary afferents can be sufficient to induce more than one modality of somatosensation, itch and pain in this case.

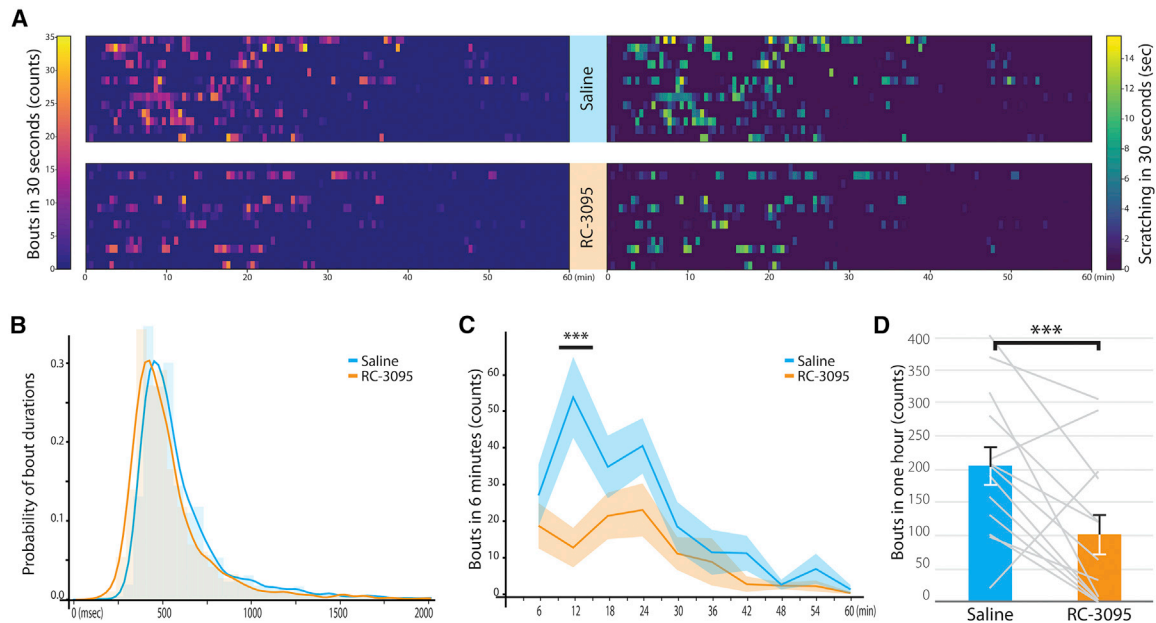


**Figure 4. Pruriception Mediated by MrgprA3 C-Afferents Is GRPR Dependent**

(A) CQ-induced itch is inhibited by the selective GRPR blocker RC-3095 (50 pmol i.c.). Shown is the time course of scratching behavior induced by CQ (10 mM) in the nape of the neck (at time = 0) 15 min after i.c. injection of saline (top) or RC-3095 (bottom). Each row represents an individual C57Bl6 mouse ( $n = 13$ ), and every block indicates the number of scratching bouts (left) or time spent scratching (right) in the corresponding 30-s bin, as defined by the color maps. (B) Similar distribution of individual scratching bout durations (552.6 and 536.7 ms on average for the saline and RC-3095 groups, respectively), despite different total counts (2,711 versus 1,348 for the saline and RC-3095 groups, respectively), indicates no significant changes in the scratching behavior phenotype. (C) Timeline of scratching behavior indicates that GRPR blockade decreases scratching at early time points. Average counts in 6-min time bins are displayed with shades indicating SEMs (two-way ANOVA test with Bonferroni post-tests). (D) Total number of scratching bouts following CQ injection indicates itch suppression by pharmacological blockade of GRPR ( $p < 0.001$ , paired t test). Each line corresponds to an individual mouse in two different conditions.

### Itch and Pain Mediated by MrgprA3 C-Afferents Engage Distinct Pathways

To verify whether the distinct behavioral responses evoked by different activation modes have unique tractable properties and network consequences, we investigated higher-order pathways recruited at the spinal cord level. To confirm the spinal pathways engaged downstream of peripheral activation of MrgprA3 C-afferents *in vivo*, we checked the involvement of GRP and its receptor, GRPR, as several studies have indicated that itch depends on the GRP-GRPR pathway in the spinal cord (Albisetti et al., 2019; Sun and Chen, 2007; Sun et al., 2009). Verifying MrgprA3 afferents' innervations to the dorsal horn of spinal cord (Figures S3A and S3B), we blocked GRPR by intra-cisternal (i.c.) administration of the GRPR antagonist RC-3095. Dye injection tests confirm that compounds administered i.c. can diffuse to the lumbar enlargement as soon as 5 min after injection. CQ was injected intra-dermally (i.d.) 15 min after i.c. administration of RC-3095 or vehicle (saline). Animals were videotaped from multiple angles for 1 h. Accurate time points for all scratching bouts were analyzed offline for generation of bout count and scratching duration heatmaps (Figure 4A). Overall similarity of the heatmaps and comparable bout duration histograms indicate qualitative similarity in the scratching behaviors in drug or vehicle conditions (Figures 4A and 4B). Analysis of the scratching time course following

GRPR inhibition reveals a decreased intensity in early time points after CQ injection (Figures 4C and S3C). Efficiency of GRPR blockade is also demonstrated by the significant decrease in total scratching bout counts and total time spent scratching during the 1-h period following CQ injection (Figures 4D and S3D).

These data confirm that a spinal GRP/GRPR-dependent pruriceptive pathway is engaged when MrgprA3 C-afferents are stimulated metabotropically through activation of native Gq-protein-coupled receptors. It is worth noting that injection of the selective mu opioid receptor agonist DAMGO i.c. did not cause a significant change in the number of scratching bouts.

To study the recruitment of similar or distinct central pathways downstream of optical activation of MrgprA3 C-afferents *in vivo*, we designed experiments for quantitative analysis of nociception based on well-established models of pain scoring in mouse hindpaws. Trafficking of ChR2 in the peripheral MrgprA3 fibers in the glabrous skin of hindpaw was confirmed by the presence of EYFP (Figure 5A) in addition to its expression validation in the lumbar DRGs and the trafficking to the central terminals in dorsal horn of the spinal cord (Figure S4). Transdermal illumination of the hindpaw induces nociceptive behaviors in the MrgprA3<sup>Cre-EGFP+/-</sup>.Rosa26<sup>ChR2-EYFP+/-</sup> mice (Video S7). These responses range from withdrawal and flinches to licking, shaking, and, rarely, vocalization. No evoked behavioral response was observed in Cre<sup>-</sup> cagemate

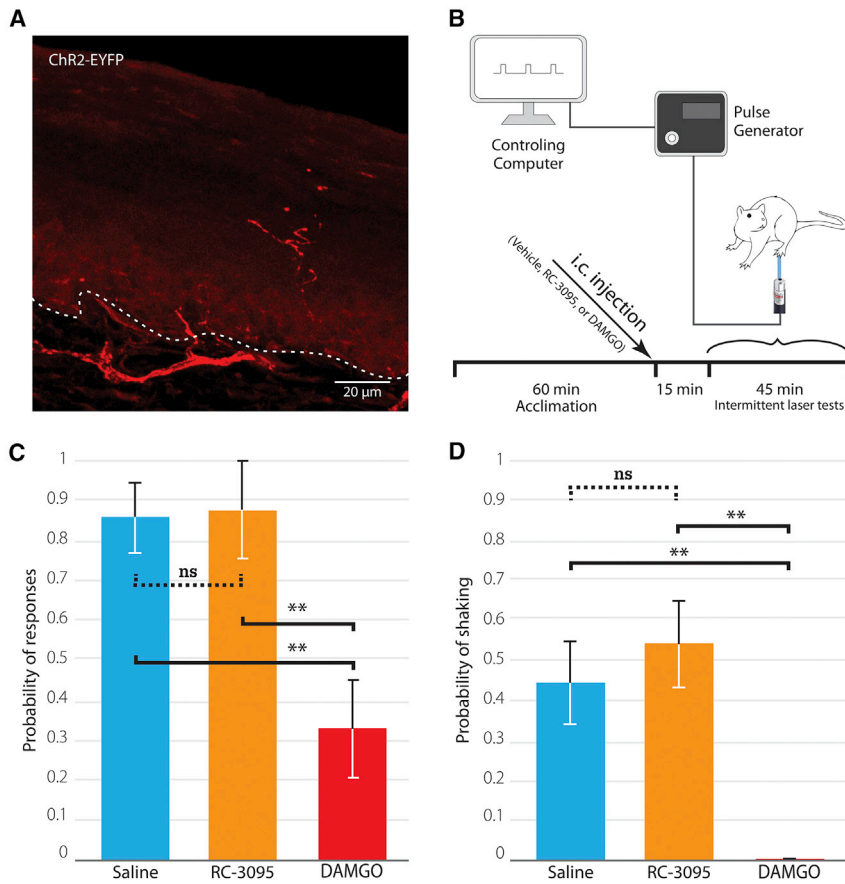


**Figure 5. Nociception Mediated by MrgprA3 C-Afferents Is Sensitive to Mu Opioid Receptor Signaling, but Not to GRPR Blockade**

(A) MrgprA3-expressing afferents innervate the glabrous skin of the paw. Representative image showing direct EYFP fluorescence in MrgprA3<sup>Cre-EGFP+/-</sup>;Rosa26<sup>ChR2-EYFP+/-</sup> animals in the plantar surface of the hindpaw. The dermis-epidermis border is indicated by a dotted line.

(B) Experimental design for quantification of optically induced pain responses. Acclimated animals received i.c. injections of 50 pmol RC-3095 or 100 pmol DAMGO 15 min before the start of optical stimulation trials (12 animals, 3 trials per treatment). (C) Probability of all evoked behavioral responses upon transdermal photostimulation of the hindpaw is not affected by GRPR blockade yet is significantly reduced by treatment with the mu opioid agonist DAMGO ( $p < 0.01$ , one-way ANOVA with Bonferroni post hoc test).

(D) Light-evoked shaking is suppressed by DAMGO, while RC-3095 does not cause any significant changes in the probability of this high-intensity pain behavior ( $p < 0.01$ , one-way ANOVA with Bonferroni post-test).

littermates after illumination of the hindpaw, eliminating concerns about possible thermal or visual effects of the laser light (Video S8). When treated with RC-3095, similarly to when they received vehicle, animals showed behavioral responses to nearly all optical stimulations (Figure 5C). On the contrary, when the animals received DAMGO, they were found to be insensitive to the majority of stimulations (Figure 5C). This difference was also evident by comparison of the probability of single behavior types such as shaking, which is linked to higher pain intensities. The lack of RC-3095 effect on shaking behavior is in contrast with the powerful suppressing effect of the opioid DAMGO (Figure 5D).

These results indicate that unlike pruriception caused by metabotropic excitation of MrgprA3 C-afferents, nociception induced by optical stimulation of these primary sensory neurons is not GRP/GRPR dependent. Furthermore, we provide evidence that, like most nocifensive responses, optically induced MrgprA3 neuron-dependent pain behavior is sensitive to opioids.

#### Calcium-Permeable TRP Channels Contribute Exclusively to the Pruriception, but Not to the Nociception, Mediated by MrgprA3 C-Afferents

Next, we investigated what molecular pathways in the MrgprA3 C-fiber neurons may be differentially involved downstream of their metabotropic (i.e., GPCRs) or ionotropic (i.e., ChR2) stimu-

lation. As TRP channels have been proposed as key components of CQ-evoked pruriception (Hill et al., 2018; Moore et al., 2018; Than et al., 2013; Wilson et al., 2011), we tested the effects of blocking sensory TRPC3, TRPA1, and TRPV1 channels with selective antagonists (Figure 6).

For the pruriception arm of this experiment, acclimated animals were injected subcutaneously with pyrazole 10, HC030031, AMG9810 (selective blockers of TRPC3, TRPA1, and TRPV1, respectively), or their vehicle, in the nape of the neck 10 min before i.d. injection of CQ. They were then videotaped for 1 h from multiple angles, and behaviors were scored offline by a blinded experimenter (Figures 6A–6D). Overlapping bout duration distribution and general similarity of bout counts and time spent scratching heatmaps suggest similar perceptual quality evoked in all groups (Figures 6A and 6B). Behavioral analysis of bout counts as well as time spent scratching indicates that all three blockers significantly decrease pruriception intensity in early time points after CQ injection (Figures 6C and S5). Notwithstanding, total counts and times of scratching for the 1-h period after CQ injection were significantly reduced only following TRPA1 and TRPV1 blockade (Figure 6D). This can be attributed to the different pharmacokinetics of the blockers or differences in the contributions of specific TRP channels to the pruriceptive signal. In agreement with previous studies, we show that the pruriception caused by chemical activation of MrgprA3 primary afferents engages calcium-permeable TRP channels.

Reciprocally, for the nociception arm of this experiment, we asked if the TRP channels are specifically linked to the itch modality or are activated regardless of stimulation mode. Habituated animals received selective TRP blocker or vehicle in both

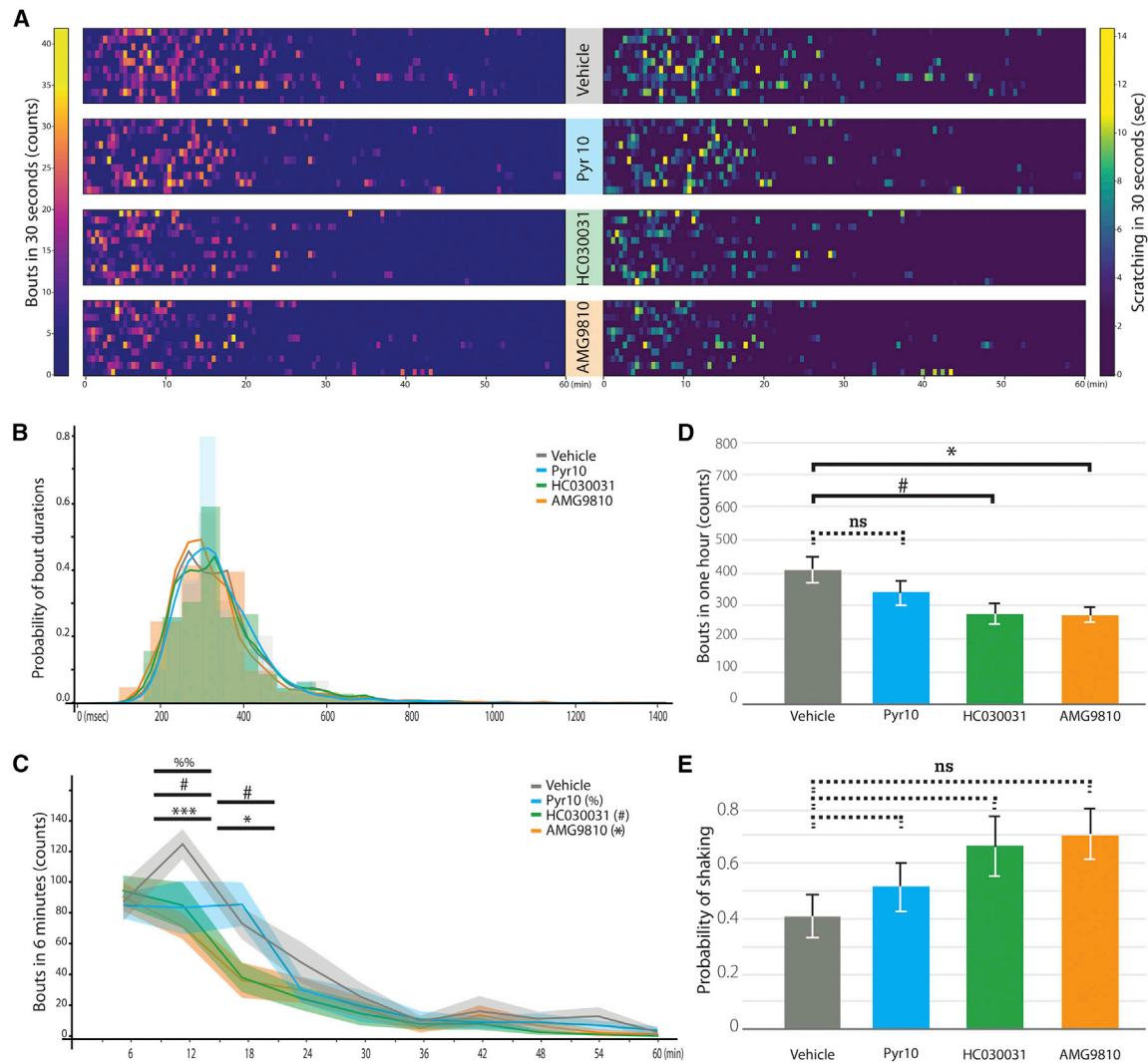


**Figure 6. Pharmacological Blockade of Peripheral TRP Channels Reduces Pruriception, but Not Nociception, Mediated by MrgprA3 C-Afferents**

(A) Time course of scratching behavior induced by injection of CQ (10 mM) in the nape of the neck (at time = 0) 10 min after subcutaneous (s.c.) injection of 1 mM solution of pyrazole 10 (Pyr10), HC030031, or AMG9810 (selective blockers of TRPC3, TRPA1, and TRPV1, respectively) or vehicle. Each line represents an individual C57Bl6 mouse ( $n = 10\text{--}11$ ), and every block indicates the number of scratching bouts (left) or time spent scratching (right) in the corresponding 30 s bin, as defined by the color maps.

(B) Probability distribution of bout durations showing similar scratching phenotypes (mean bout durations of 356.0, 348.9, 347.2, and 339.4 ms for vehicle, Pyr10, HC030031, and AMG9810, respectively).

(C) Timeline of scratching counts after injection of CQ (at time = 0) in animals pretreated by selective TRP channel blockers (at time = 10 min) (two-way ANOVA with Bonferroni post hoc test; %, #, and \* symbols depict significance levels for comparison of the vehicle versus the Pyr10, HC030031, or AMG9810 group, respectively).

(D) Total number of scratching bouts in the 1-h period following CQ injection shows that pharmacological blockade of TRPA1 or TRPV1 channels inhibits the pruriception triggered by MrgprA3 C-afferents (one-way ANOVA with Bonferroni post hoc test).

(E) The probability of shaking behavior induced by photostimulation of the hindpaw, as a readout for pain, indicates that pretreatment of MrgprA3<sup>Cre-EGFP+/-</sup>; Rosa26<sup>ChR2-EYFP+/-</sup> animals with TRP channel blockers does not inhibit light-evoked nociception ( $n = 9$ , one-way ANOVA with Bonferroni post hoc test).

hindpaws 10 min before intermittent pulses of 470-nm (blue) laser were applied to their glabrous skin. Unlike the opioidergic intervention on the central terminals with DAMGO described previously (Figure 5), there were no significant changes observed after peripheral blockade of the TRP channels TRPC3, TRPV1, or TRPA1. In all instances of optical stimulation, the animals mani-

fested nocifensive responses, and expression of higher-intensity behaviors such as shaking did not show any significant decrease (Figure 6E). We conclude from these observations that calcium-permeable TRPC3, TRPA1, and TRPV1 channels do not contribute significantly to the pain signaling pathway downstream of optical activation of MrgprA3 C-afferents.

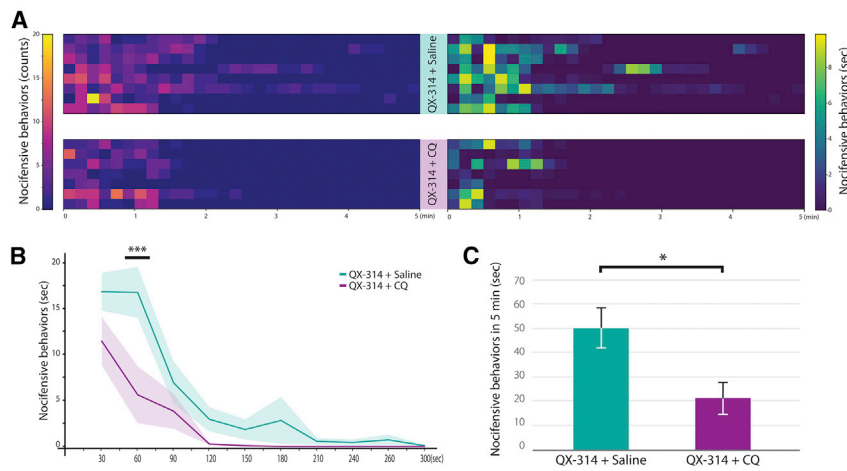


**Figure 7. Selective Silencing of MrgprA3 C-Afferents Significantly Reduces Acute Purinergic Pain**

(A) Time course of nocifensive behavior induced by intraplantar injection of  $\alpha\beta$ meATP (20 mM) in the hindpaw 30 min after conditioning with coinjection of QX-314 with saline or CQ (5 mM). Each line represents an individual wild-type C57Bl6 mouse ( $n = 7-8$ ), and every block indicates the number of lifting or licking behaviors observed (left panel) or time spent behaving (right panel) in 10-s time bins, as defined by the heatmaps.

(B) Timeline of nocifensive behaviors observed (lifting and licking), showing that QX-314-mediated silencing of the CQ-responsive cells blunts the expression of nocifensive behaviors evoked by  $\alpha\beta$  meATP. Average durations in 30-s time bins are displayed with shades indicating SEMs. Two-way ANOVA with Bonferroni post tests were used for statistical comparison ( $p < 0.001$ ).

(C) Conditional silencing of CQ-responsive afferents reduces the total duration of purinergic nocifensive behaviors. Animals receiving QX-314 + CQ 30 min before  $\alpha\beta$ meATP spend significantly less time manifesting nocifensive behaviors (licking and lifting their paw) in the 5-min period after algogen injection ( $p < 0.05$ , unpaired t test).

Collectively, these results indicate that TRP channels expressed in MrgprA3 C-afferents are engaged in itch transduction but are not recruited in optically induced nociceptive transduction.

### MrgprA3 C-Afferents Contribute to Acute Pain Responses in Wild-Type Mice

To assess the contribution of MrgprA3 C-afferents to pain in more naturalistic conditions and in non-transgenic wild-type mice, we studied the behavioral effect of their fast ionotropic stimulation through the activation of native cation channels. We took advantage of the fact that most nonpeptidergic C-afferents, including the MrgprA3 subset, express P2X3 ATP-gated channels (Usoskin et al., 2015). It has been shown that application of the P2X3 agonist  $\alpha,\beta$ -methylene ATP ( $\alpha\beta$ meATP) in rats and mice induces pain (Bland-Ward and Humphrey, 1997; Kakimoto et al., 2008; Kato et al., 2002; Tsuda et al., 2002). We confirmed that the nocifensive behavioral responses evoked by selective P2X agonists consists of lifting and licking, manifested chiefly in the first 5 min after injection in the hindpaw. These responses are similar to that of nocifensive ChR2-evoked responses in MrgprA3<sup>Cre-EGFP+/-</sup>; Rosa26<sup>ChR2-EYFP+/-</sup> mice (Figure 5). To study the contribution of MrgprA3-expressing afferents to  $\alpha\beta$ meATP-induced pain, we used the approach of conditional activity-dependent silencing with QX-314. It has previously shown that CQ effectively induces the influx of QX-314 in MrgprA3 neurons, resulting in their silencing (Roberson et al., 2013). Acclimated wild-type C57Bl6 mice were placed on the testing platform for at least 30 min before receiving a conditioning intraplantar coinjection of 5 mM CQ and 1% QX-314 or a control solution of saline and 1% QX-314. 30 min after conditioning, 10  $\mu$ L of 20 mM  $\alpha\beta$ meATP was administered to the same hindpaw. Total counts and time spent licking or lifting the injected hindpaw in every 10-s bin after injection is visualized in separate heatmaps (Figure 7A). Temporal progression of the total time spent behaving shows significantly higher intensities of nociceptive behavior in controls compared to the QX-314 + CQ group (Figure 7B). The total duration of time spent manifesting nocifensive responses over the 5 min after  $\alpha\beta$ meATP injection also indi-

cates a significant decrease when the MrgprA3 C-afferents were silenced with QX-314 + CQ (Figure 7C). Separate analysis of lifting and licking responses show similar reduction in the QX-314 + CQ group compared to that of the QX-314 + saline group (Figure S6).

We conclude that MrgprA3 C-afferents significantly contribute to the acute pain behavior caused by  $\alpha\beta$ meATP injection as their silencing results in decreased nociceptive responses in this model. These data support our hypothesis that in specific conditions, such as optogenetic or naturally occurring fast purinergic ionotropic stimulations, these C-fibers can convey pain signals.

## DISCUSSION

Taking advantage of cell-type-selective stimulation techniques, we provide evidence that a single genetically determined population of peripheral afferents, the MrgprA3 subset previously proposed as a labeled line for itch, is sufficient for coding both itch and pain signals. Regardless of their genetic labeling, we also show that CQ-responsive afferents can signal both acute prurceptive and nociceptive stimuli in natural conditions. We further demonstrate that these neurons exhibit their multimodal properties by recruiting specific ion channels and by engaging divergent pathways in the spinal cord. Challenging the labeled line theory, our data support the concept that somatosensory discrimination can be initiated at the peripheral level in primary afferents through cell-autonomous mechanisms.

In order to dissect functional contribution of primary sensory afferents to somatosensation, various methods of genetic and morphological categorization have been implemented (Le Pichon and Chesler, 2014; Usoskin et al., 2015; Zeisel et al., 2018). Basic molecular and functional characterization of MrgprA3 C-afferents provides hints of their multimodality, as this neuronal subset does not fit in any single conventional category of primary afferents (e.g., peptidergic versus non-peptidergic, mechano-sensitive versus heat sensitive, or nociceptors versus pruriceptors). Indeed,  $\sim 85\%$  of MrgprA3 neurons express the peptidergic marker CGRP, while  $\sim 80\%$  express the

non-peptidergic marker IB4, and ~85% express P2X3 ATP receptors. They display electrophysiological properties of C-mechanoheat (CMH) nociceptors and respond to histamine, capsaicin, CQ, and cowhage (Han et al., 2013). Thus, in addition to cellular categorizations, we propose recognizing their mode of stimulation. For controlled comparisons, we chose to engage MrgprA3<sup>+</sup> cells through either the native metabotropic actuator MrgprA3 or the heterologous ionotropic actuator ChR2. We ensured access to the same population of neurons and co-expression of ChR2 and MrgprA3 by crossing the MrgprA3-Cre driver with Cre-dependent actuator lines, as almost-perfect co-expression of reporters (over 96%) has been previously established (Han et al., 2013; Tang et al., 2016). Furthermore, independently from any genetic targeting intervention, we present evidence that CQ-responsive afferents convey itch (Figures 1 and 3), while the same pharmacologically identified afferents contribute to pain coding (Figure 7). Therefore, different modes of stimulation induce distinct behaviors reflecting different sensory modalities with distinct pharmacological characteristics consistent with the perception of pain and itch. We also report that coding itch modality is independent of the size of the MrgprA3 afferent population recruited, since stimulation of only a fraction of these cells through virally transduced DREADDs generates stereotypical itch responses qualitatively identical to behaviors evoked by their global activation through endogenous MrgprA3 receptors, yet with lower intensity.

Quantitative animal behavioral assays have significantly improved our understanding of itch as a sensory modality (Dong and Dong, 2018; LaMotte et al., 2011). Using a detailed quantitative method, we confirm the “waxing and waning” of itch (Forster and Handwerker, 2014). In addition to measuring itch intensity with scratching bout counts or time spent scratching, individual scratching bout durations can also be used to describe itch perception. Considering the complex nature of pruritus, with multiple initiation mechanisms (Green and Dong, 2016; Han and Simon, 2011; Luo et al., 2015), cellular/molecular diversity (Bautista et al., 2014; Song et al., 2018), and behavioral itch-scratch cycles (Mack and Kim, 2018), we believe analyzing and presenting scratching data over time improves detection and comparison between interventions. We also used a quantitative approach toward behavioral analysis of nociception, because animals present various responses to painful stimuli at various locations on their body. Therefore, we measured all nocifensive responses as well as intense-pain behaviors like shaking for pain quantification (Figures 5 and 6). A lack of sensitivity may be the main cause for not observing significant pain reduction following ablation or inactivation of small subsets of C-afferents such as MrgprA3<sup>+</sup> cells representing less than 10% of DRG neurons (Han et al., 2013; Liu et al., 2009). Proving that with appropriate readouts the MrgprA3 afferents' contribution to acute nociception is detectable, our results further show that in specific conditions, their stimulation can be sufficient to evoke nocifensive behaviors.

Although pruriceptive and nocifensive behaviors have been characterized in mice in different assays, not all behavioral manifestations are associated with either itch or pain, like grooming in the cheek assay (Shimada and LaMotte, 2008). An unbiased characterization of behavioral responses is particularly important when it comes to testing the effects of unnatural stimuli

such as optical stimulations in optogenetic experiments. This could be one main cause of discrepancy between our results and data by Sun et al. (2017) showing induction of itch and no pain upon transdermal photostimulation of MrgprA3 fibers. We quantified all responses that were elicited by laser illumination on the neck, including (but not limited to) scratching, and measured uncategorized aversive behaviors separately. It is also important to consider that itch responses directed to different areas of the body can differ, such as hindpaw scratching of the cheek but rapid biting of the calf in response to pruriception (LaMotte et al., 2011). This is partly due to anatomical constraints, such as not reaching the nape with the forepaw and precluding wiping behavior upon neck illumination as mentioned by Sun et al. (2017). We believe that in experiments without stabilized optical sources, uncontrolled illumination site and power, due to moving targets, is a source of discrepancy in interpreting results. That is why we chose to use the cheek assay (Shimada and LaMotte, 2008) with constant stimulation field. Our unambiguous results with the cheek assay, and the fact that on three different body areas (neck, cheek, and hindpaw), we did not observe predominant stereotypical itch behaviors (hindpaw scratching or biting), support our conclusion that optical stimulation of MrgprA3 C-afferents triggers pain and not itch. We further validated the distinct perception of itch or pain based on their specific sensitivity to known pharmacological anti-pruritic or analgesic interventions.

TRP channels have been identified as transducers downstream of metabotropic receptors for pruritogens (Dong and Dong, 2018; Feng et al., 2017; Moore et al., 2018; Xie and Hu, 2018). TRPA1 and TRPC3 have been shown to play a significant role in the activation of primary afferents by CQ (Than et al., 2013; Wilson et al., 2011), while action potential generation induced by CQ did not seem to be altered in a constitutive double knockout of TRPV1 and TRPA1 in an *ex vivo* preparation (Ru et al., 2017). *In vivo*, however, constitutive TRPA1 knockout animals exhibit shorter total scratching time following CQ injection, while constitutive TRPV1 knockout animals show typical duration of scratching (Wilson et al., 2011). On the other hand, it has been shown that CQ sensitizes TRPV1 channels in MrgprA3 neurons (Than et al., 2013). Our data on the exclusive involvement of TRP channels in pruriception also confirms the capability of MrgprA3 C-afferents to respond distinctively to different stimuli in a cell-autonomous manner. The differential coding of algescic and pruritic stimuli mediated by these afferents may be carried by distinct firing patterns or secondary messengers, resulting in distinct neurochemical or temporal outputs in their central terminals (Hong et al., 2012; Ratté et al., 2013; Wang et al., 2017; Zeldenrust et al., 2018). These biased responses engage separate pathways in the spinal cord, as shown here by the differential sensitivity of MrgprA3 neuron-mediated itch and pain responses to the GRPR antagonist RC-3095 and the mu opioid receptor agonist DAMGO, respectively. Differential spinal integration of signals transmitted by a single peripheral neuronal population likely depends on spatiotemporal properties of its outputs, where short synchronous ionotropic signals can carry different messages than longer asynchronous metabotropic signals. Whereas slow sporadic asynchronous signals evoked by chemical activation of MrgprA3 C-afferents favors pruriception (Han et al., 2013), our results suggest that fast synchronous signals

evoked by optogenetic or purinergic stimulation of these same C-fibers favors nociception. Another contributing factor to the spatiotemporal signature of central outputs is the afferents firing patterns. Indeed, spinal GRP interneurons can engage both pain and itch pathways (Sun et al., 2017), and they require burst-like activity in order to relay pruriceptive signals to higher-order neurons (Pagani et al., 2019). Our data indicate that primary afferents can also transmit distinct modality-specific signals to the spinal cord. For instance, single action potentials versus the burst-like firing pattern generated by MrgprA3 afferents could differentially code for pain versus itch modalities.

Similar principles of multimodal coding based on stimulation conditions will likely be observed in other sensory circuits. Furthermore, beyond the field of sensory neurobiology and in view of the widespread use of heterologous actuators in modern neuroscience, this study provides evidence that fast ionotropic and slower metabotropic stimulation of the same genetically defined populations of neurons can lead to different outcomes at cellular and behavioral levels.

## STAR★METHODS

Detailed methods are provided in the online version of this paper and include the following:

- KEY RESOURCES TABLE
- RESOURCE AVAILABILITY
  - Lead Contact
  - Materials Availability
  - Data and Code Availability
- EXPERIMENTAL MODEL AND SUBJECT DETAILS
  - Mouse strains
  - Primary neuron cultures
- METHOD DETAILS
  - Ligands and administration routes
  - Viral constructs and transduction
  - Headpost implants
  - Laser sources and light guides
  - Behavioral assays
  - *In vitro* preparations and assays
  - *Ex vivo* tissue preparations and morphology
- QUANTIFICATION AND STATISTICAL ANALYSIS

## SUPPLEMENTAL INFORMATION

Supplemental Information can be found online at <https://doi.org/10.1016/j.neuron.2020.03.021>.

## ACKNOWLEDGMENTS

We thank our McGill colleagues Jeffrey Mogil and Stuart Trenholm for their input, Xinzhong Dong (Johns Hopkins, HHMI) for the MrgprA3-Cre-EGFP mouse line, and Van Vn Nguyen for her technical support. B.S. received scholarships from the Fonds de Recherche du Québec - Santé and the Louise and Alan Edwards Foundation. This work was funded by the Canadian Institutes of Health Research (A.R.-d.-S. and P.S.), the Natural Sciences and Engineering Research Council of Canada (P.S.), the Quebec Pain Research Network (A.R.-d.-S. and P.S.), and the Louise and Alan Edwards Foundation (A.R.-d.-S. and P.S.).

## AUTHOR CONTRIBUTIONS

B.S. and P.S. designed the experiments and all authors contributed to data analysis. B.S. performed the histological characterization with A.R.-d.-S. B.S. conducted the calcium imaging and the behavioral experiments. A.R.A. and B.S. performed the electrophysiological experiments. B.S. and P.S. wrote the paper, with contributions from all authors. P.S. supervised all aspects of the work.

## DECLARATION OF INTERESTS

The authors declare no competing interests.

Received: June 20, 2019

Revised: October 21, 2019

Accepted: March 20, 2020

Published: April 15, 2020

## REFERENCES

- Albisetti, G.W., Pagani, M., Platonova, E., Hösl, L., Johannssen, H.C., Fritschy, J.-M., Wildner, H., and Zeilhofer, H.U. (2019). Dorsal horn gastrin-releasing peptide expressing neurons transmit spinal itch but not pain signals. *J. Neurosci.* *39*, 2238–2250.
- Bautista, D.M., Wilson, S.R., and Hoon, M.A. (2014). Why we scratch an itch: the molecules, cells and circuits of itch. *Nat. Neurosci.* *17*, 175–182.
- Bland-Ward, P.A., and Humphrey, P.P. (1997). Acute nociception mediated by hindpaw P2X receptor activation in the rat. *Br. J. Pharmacol.* *122*, 365–371.
- Brull, S.J., Atanassoff, P.G., Silverman, D.G., Zhang, J., and Lamotte, R.H. (1999). Attenuation of experimental pruritus and mechanically evoked dysesthesiae in an area of cutaneous allodynia. *Somatosens. Mot. Res.* *16*, 299–303.
- Daou, I., Tuttle, A.H., Longo, G., Wieskopf, J.S., Bonin, R.P., Ase, A.R., Wood, J.N., De Koninck, Y., Ribeiro-da-Silva, A., Mogil, J.S., and Séguéla, P. (2013). Remote optogenetic activation and sensitization of pain pathways in freely moving mice. *J. Neurosci.* *33*, 18631–18640.
- Davidson, S., and Giesler, G.J. (2010). The multiple pathways for itch and their interactions with pain. *Trends Neurosci.* *33*, 550–558.
- Dong, X., and Dong, X. (2018). Peripheral and central mechanisms of itch. *Neuron* *98*, 482–494.
- Dong, X., Han, S., Zylka, M.J., Simon, M.I., and Anderson, D.J. (2001). A diverse family of GPCRs expressed in specific subsets of nociceptive sensory neurons. *Cell* *106*, 619–632.
- Feng, J., Yang, P., Mack, M.R., Dryn, D., Luo, J., Gong, X., Liu, S., Oetjen, L.K., Zholos, A.V., Mei, Z., et al. (2017). Sensory TRP channels contribute differentially to skin inflammation and persistent itch. *Nat. Commun.* *8*, 980.
- Forster, C., and Handwerker, H.O. (2014). Central nervous processing of itch and pain. In *Itch: Mechanisms and Treatment, Chapter 24*, E. Carstens and T. Akiyama, eds. (CRC Press/Taylor & Francis).
- Green, D., and Dong, X. (2016). The cell biology of acute itch. *J. Cell Biol.* *213*, 155–161.
- Green, A.D., Young, K.K., Lehto, S.G., Smith, S.B., and Mogil, J.S. (2006). Influence of genotype, dose and sex on pruritogen-induced scratching behavior in the mouse. *Pain* *124*, 50–58.
- Han, S.-K., and Simon, M.I. (2011). Intracellular signaling and the origins of the sensations of itch and pain. *Sci. Signal.* *4*, pe38.
- Han, L., Ma, C., Liu, Q., Weng, H.-J., Cui, Y., Tang, Z., Kim, Y., Nie, H., Qu, L., Patel, K.N., et al. (2013). A subpopulation of nociceptors specifically linked to itch. *Nat. Neurosci.* *16*, 174–182.
- Hill, R.Z., Morita, T., Brem, R.B., and Bautista, D.M. (2018). S1PR3 mediates itch and pain via distinct TRP channel-dependent pathways. *J. Neurosci.* *38*, 7833–7843.
- Hong, S., Ratté, S., Prescott, S.A., and De Schutter, E. (2012). Single neuron firing properties impact correlation-based population coding. *J. Neurosci.* *32*, 1413–1428.

- Kakimoto, S., Nagakura, Y., Tamura, S., Watabiki, T., Shibasaki, K., Tanaka, S., Mori, M., Sasamata, M., and Okada, M. (2008). Minodronic acid, a third-generation bisphosphonate, antagonizes purinergic P2X(2/3) receptor function and exerts an analgesic effect in pain models. *Eur. J. Pharmacol.* **589**, 98–101.
- Kato, A., Ohkubo, T., and Kitamura, K. (2002). Allogene-specific pain processing in mouse spinal cord: differential involvement of voltage-dependent Ca(2+) channels in synaptic transmission. *Br. J. Pharmacol.* **135**, 1336–1342.
- Klein, A., Carstens, M.I., and Carstens, E. (2011). Facial injections of pruritogens or algogens elicit distinct behavior responses in rats and excite overlapping populations of primary sensory and trigeminal subnucleus caudalis neurons. *J. Neurophysiol.* **106**, 1078–1088.
- LaMotte, R.H., Shimada, S.G., and Sikand, P. (2011). Mouse models of acute, chemical itch and pain in humans. *Exp. Dermatol.* **20**, 778–782.
- LaMotte, R.H., Dong, X., and Ringkamp, M. (2014). Sensory neurons and circuits mediating itch. *Nat. Rev. Neurosci.* **15**, 19–31.
- Le Pichon, C.E., and Chesler, A.T. (2014). The functional and anatomical dissection of somatosensory subpopulations using mouse genetics. *Front. Neuroanat.* **8**, 21.
- Lembo, P.M.C., Grazzini, E., Groblewski, T., O'Donnell, D., Roy, M.-O., Zhang, J., Hoffer, C., Cao, J., Schmidt, R., Pelletier, M., et al. (2002). Proenkephalin A gene products activate a new family of sensory neuron-specific GPCRs. *Nat. Neurosci.* **5**, 201–209.
- Liu, Q., Tang, Z., Surdenikova, L., Kim, S., Patel, K.N., Kim, A., Ru, F., Guan, Y., Weng, H.-J., Geng, Y., et al. (2009). Sensory neuron-specific GPCR Mrgpr8 are itch receptors mediating chloroquine-induced pruritus. *Cell* **139**, 1353–1365.
- Liu, Q., Sikand, P., Ma, C., Tang, Z., Han, L., Li, Z., Sun, S., LaMotte, R.H., and Dong, X. (2012). Mechanisms of itch evoked by  $\beta$ -alanine. *J. Neurosci.* **32**, 14532–14537.
- Luo, J., Feng, J., Liu, S., Walters, E.T., and Hu, H. (2015). Molecular and cellular mechanisms that initiate pain and itch. *Cell. Mol. Life Sci.* **72**, 3201–3223.
- Mack, M.R., and Kim, B.S. (2018). The itch-scratch cycle: a neuroimmune perspective. *Trends Immunol.* **39**, 980–991.
- McMahon, S.B., and Koltzenburg, M. (1992). Itching for an explanation. *Trends Neurosci.* **15**, 497–501.
- Moore, C., Gupta, R., Jordt, S.-E., Chen, Y., and Liedtke, W.B. (2018). Regulation of pain and itch by TRP channels. *Neurosci. Bull.* **34**, 120–142.
- Nilsson, H.J., Levinsson, A., and Schouenborg, J. (1997). Cutaneous field stimulation (CFS): a new powerful method to combat itch. *Pain* **71**, 49–55.
- Pagani, M., Albisetti, G.W., Sivakumar, N., Wildner, H., Santello, M., Johannsen, H.C., and Zeilhofer, H.U. (2019). How gastrin-releasing peptide opens the spinal gate for itch. *Neuron* **103**, 102–117.e5.
- Ratté, S., Hong, S., De Schutter, E., and Prescott, S.A. (2013). Impact of neuronal properties on network coding: roles of spike initiation dynamics and robust synchrony transfer. *Neuron* **78**, 758–772.
- Roberson, D.P., Gudes, S., Sprague, J.M., Patoski, H.A.W., Robson, V.K., Blasl, F., Duan, B., Oh, S.B., Bean, B.P., Ma, Q., et al. (2013). Activity-dependent silencing reveals functionally distinct itch-generating sensory neurons. *Nat. Neurosci.* **16**, 910–918.
- Ru, F., Sun, H., Jurcakova, D., Herbtsomer, R.A., Meixong, J., Dong, X., and Udem, B.J. (2017). Mechanisms of pruritogen-induced activation of itch nerves in isolated mouse skin. *J. Physiol.* **595**, 3651–3666.
- Scherrer, G., Imamachi, N., Cao, Y.-Q., Contet, C., Mennicken, F., O'Donnell, D., Kieffer, B.L., and Basbaum, A.I. (2009). Dissociation of the opioid receptor mechanisms that control mechanical and heat pain. *Cell* **137**, 1148–1159.
- Schmelz, M. (2015). Itch and pain differences and commonalities. *Handb. Exp. Pharmacol.* **227**, 285–301.
- Shimada, S.G., and LaMotte, R.H. (2008). Behavioral differentiation between itch and pain in mouse. *Pain* **139**, 681–687.
- Simone, D.A., Zhang, X., Li, J., Zhang, J.-M., Honda, C.N., LaMotte, R.H., and Giesler, G.J., Jr. (2004). Comparison of responses of primate spinothalamic tract neurons to pruritic and algogenic stimuli. *J. Neurophysiol.* **91**, 213–222.
- Song, J., Xian, D., Yang, L., Xiong, X., Lai, R., and Zhong, J. (2018). Pruritus: progress toward pathogenesis and treatment. *BioMed Res. Int.* **2018**, 9625936.
- St Sauver, J.L., Warner, D.O., Yawn, B.P., Jacobson, D.J., McGree, M.E., Pankratz, J.J., Melton, L.J., 3rd, Roger, V.L., Ebbert, J.O., and Rocca, W.A. (2013). Why patients visit their doctors: assessing the most prevalent conditions in a defined American population. *Mayo Clin. Proc.* **88**, 56–67.
- Stantcheva, K.K., Iovino, L., Dhandapani, R., Martinez, C., Castaldi, L., Nocchi, L., Perlas, E., Portulano, C., Pesaresi, M., Shirlekar, K.S., et al. (2016). A subpopulation of itch-sensing neurons marked by Ret and somatostatin expression. *EMBO Rep.* **17**, 585–600.
- Sun, Y.-G., and Chen, Z.-F. (2007). A gastrin-releasing peptide receptor mediates the itch sensation in the spinal cord. *Nature* **448**, 700–703.
- Sun, Y.-G., Zhao, Z.-Q., Meng, X.-L., Yin, J., Liu, X.-Y., and Chen, Z.-F. (2009). Cellular basis of itch sensation. *Science* **325**, 1531–1534.
- Sun, S., Xu, Q., Guo, C., Guan, Y., Liu, Q., and Dong, X. (2017). Leaky gate model: intensity-dependent coding of pain and itch in the spinal cord. *Neuron* **93**, 840–853.e5.
- Tang, M., Wu, G., Wang, Z., Yang, N., Shi, H., He, Q., Zhu, C., Yang, Y., Yu, G., Wang, C., et al. (2016). Voltage-gated potassium channels involved in regulation of physiological function in MrgprA3-specific itch neurons. *Brain Res.* **1636**, 161–171.
- Than, J.Y.-X.L., Li, L., Hasan, R., and Zhang, X. (2013). Excitation and modulation of TRPA1, TRPV1, and TRPM8 channel-expressing sensory neurons by the pruritogen chloroquine. *J. Biol. Chem.* **288**, 12818–12827.
- Tsuda, M., Shigemoto-Mogami, Y., Ueno, S., Koizumi, S., Ueda, H., Iwanaga, T., and Inoue, K. (2002). Downregulation of P2X3 receptor-dependent sensory functions in A/J inbred mouse strain. *Eur. J. Neurosci.* **15**, 1444–1450.
- Ueda, H., Amano, H., Shiomi, H., and Takagi, H. (1979). Comparison of the analgesic effects of various opioid peptides by a newly devised intracisternal injection technique in conscious mice. *Eur. J. Pharmacol.* **56**, 265–268.
- Urban, D.J., and Roth, B.L. (2015). DREADDs (designer receptors exclusively activated by designer drugs): chemogenetic tools with therapeutic utility. *Annu. Rev. Pharmacol. Toxicol.* **55**, 399–417.
- Usofski, D., Furlan, A., Islam, S., Abdo, H., Lönnerberg, P., Lou, D., Hjerling-Leffler, J., Haeggström, J., Kharchenko, O., Kharchenko, P.V., et al. (2015). Unbiased classification of sensory neuron types by large-scale single-cell RNA sequencing. *Nat. Neurosci.* **18**, 145–153.
- Vos, T., Allen, C., and Arora, M.; GBD 2015 Disease and Injury Incidence and Prevalence Collaborators (2016). Global, regional, and national incidence, prevalence, and years lived with disability for 310 diseases and injuries, 1990–2015: a systematic analysis for the Global Burden of Disease Study 2015. *Lancet* **388**, 1545–1602.
- Wang, Y., Wu, Q., Hu, M., Liu, B., Chai, Z., Huang, R., Wang, Y., Xu, H., Zhou, L., Zheng, L., et al. (2017). Ligand- and voltage-gated Ca<sup>2+</sup> channels differentially regulate the mode of vesicular neuropeptide release in mammalian sensory neurons. *Sci. Signal.* **10**, eaal1683.
- Wilson, S.R., Gerhold, K.A., Bifolck-Fisher, A., Liu, Q., Patel, K.N., Dong, X., and Bautista, D.M. (2011). TRPA1 is required for histamine-independent, Mas-related G protein-coupled receptor-mediated itch. *Nat. Neurosci.* **14**, 595–602.
- Xie, Z., and Hu, H. (2018). TRP channels as drug targets to relieve itch. *Pharmaceuticals (Basel)* **11**, E100.
- Zeisel, A., Hochgerner, H., Lönnerberg, P., Johnsson, A., Memic, F., van der Zwan, J., Häring, M., Braun, E., Borm, L.E., La Manno, G., et al. (2018). Molecular architecture of the mouse nervous system. *Cell* **174**, 999–1014.e22.
- Zeldenrust, F., Wadman, W.J., and Englitz, B. (2018). Neural coding with bursts-current state and future perspectives. *Front. Comput. Neurosci.* **12**, 48.
- Zylka, M.J., Dong, X., Southwell, A.L., and Anderson, D.J. (2003). Atypical expansion in mice of the sensory neuron-specific Mrg G protein-coupled receptor family. *Proc. Natl. Acad. Sci. USA* **100**, 10043–10048.

## STAR★METHODS

### KEY RESOURCES TABLE

REAGENT or RESOURCE	SOURCE	IDENTIFIER
<b>Antibodies</b>		
PGP9.5	Ultrasclone	Cat# RA95101; RRID: AB_2313685
mCherry	Thermo Fisher Scientific	Cat# M11217; RRID: AB_2536611
<b>Bacterial and Virus Strains</b>		
AAV9-hSYN-DIO-hM3D(Gq)-mCherry (DREADD)	Bryan Roth (UNC)	RRID: Addgene_44361
<b>Chemicals, Peptides, and Recombinant Proteins</b>		
Chloroquine diphosphate	Sigma	Cat# C6628
Clozapine N-Oxide	Tocris	Cat# 4936
RC-3095	Adooq	Cat# A12753
DAMGO	Tocris	Cat# 1171
HC-030031	Tocris	Cat# 2896
AMG9810	Tocris	Cat# 2316
Pyrazole 10	Sigma	Cat# SML1243
$\alpha\beta$ meATP	Tocris	Cat# 3209
QX-314	Abcam	Cat# Ab144493
<b>Experimental Models: Organisms/Strains</b>		
Wildtype C57Bl6 Mice	Charles River Canada	C57Bl6
ChR2-EYFP Mice	Jackson Laboratory	Ai32
MrgprA3-Cre-EGFP Mice	Xinzhong Dong (JHU)	N/A

### RESOURCE AVAILABILITY

#### Lead Contact

Further information and requests for resources and reagents should be directed to and will be fulfilled by the Lead Contact, Philippe Séguéla ([philippe.seguela@mcgill.ca](mailto:philippe.seguela@mcgill.ca)).

#### Materials Availability

This study did not generate new unique reagents.

#### Data and Code Availability

This study did not generate any unique datasets or code.

### EXPERIMENTAL MODEL AND SUBJECT DETAILS

#### Mouse strains

All animal procedures were approved by the McGill animal care committee and in compliance with the Canadian Council on Animal Care guidelines. Mice were kept in 12-hour light-dark cycle, 22°C air-filtered cages (194 mm x 178 mm x 397 mm) in groups up to 5 per cage with access to food and water *ad libitum*. All animals (male, 3-10 weeks) were kept at least for 10 days in their home cages before any procedures.

Wild-type C57Bl6 mice (Charles River Canada) were used for heterozygous breedings or behavioral tests at 3-4 weeks of age. The transgenic MrgprA3<sup>Cre-EGFP</sup> mouse line was kindly provided by Xinzhong Dong (Johns Hopkins University, HHMI). Hemizygotes were bred in house by crossing to wild-type C57Bl6. The Ai32 mouse line (JAX) was used as the optogenetic reporter line, homozygotes were bred in-house.

#### Primary neuron cultures

Trigeminal ganglia (TG) or dorsal root ganglia (DRG) were dissected from adult male mice for primary culture and *in vitro* assays. In short, the animals were decapitated under isoflurane anesthesia, the sensory ganglia were removed and stored in ice-cold HBSS

solution (Invitrogen). After treating with dispase (1.4 mg/mL, Sigma) and collagenase type II (1.1 mg/mL, Sigma) for 45 min on a shaker (37°C), ganglia were washed twice with 10 mL of F-12 media (Invitrogen) containing 10% FBS, 1% L-glutamine, 1% penicillin and 1% streptomycin. The ganglia were then triturated using fire polished glass pipets with incrementally decreasing tip sizes. Dishes (35 mm) with 14 mm glass centers (MatTek) were coated with laminin (BD Biosciences) and poly-D-lysine (Sigma) for at least 2 h at 4°C. Cells were then plated for at least one hour in the incubator (37°C, 5% CO<sub>2</sub>) before addition of 2 mL culture medium. Cultured cells were used for calcium imaging or electrophysiology 24-48 hours post-plating.

## METHOD DETAILS

### Ligands and administration routes

Intra-dermal (i.d.) injections (20 µL, unless otherwise specified) were made either in the cheek or in the nape of the neck using low volume insulin syringes (Becton Dickinson). Intra-cisternal (i.c.) injections were made in 5 µL volumes using a bent 30G syringe tips (Becton Dickinson) attached to a 10 µL Hamilton syringe (Ueda et al., 1979). Intra-plantar and subcutaneous (s.c.) injections were made in 10 µL volumes and 50 µL respectively, using insulin syringes (Becton Dickinson).

Chloroquine diphosphate (Sigma) was prepared in 100 mM stock solution in deionized distilled water and was kept in aliquots at –20°C before dilution in saline (*in vivo* tests) or extracellular recording solution (*in vitro* tests). CNO (Tocris) was prepared in 5 mg/mL stock solution in deionized distilled water and was kept in aliquots at –80°C before dilution in saline (*in vivo* tests) or extracellular recording solution (*in vitro* tests). RC3095 (Adooq Bioscience) was prepared in 10 mM stock solution in deionized distilled water and was kept in aliquots at –80°C before dilution in saline for i.c. injections. DAMGO (Tocris) was prepared in 1 mM stock solution in deionized distilled water and was kept in aliquots at –80°C before dilution in saline. TRP channel blockers pyrazole 10 (Sigma), HC-030031 (Tocris), and AMG9810 (Tocris), were prepared in 5 mM stock solutions and stored at –20°C in aliquots before dilution to the final concentration of 1 mM in 10% ethanol and 10% DMSO at the time of experiments.  $\alpha,\beta$ -methylene adenosine 5'-triphosphate trisodium salt ( $\alpha\beta$ meATP, Tocris) was prepared in 20 mM stock solution in saline and was kept in aliquots at –20°C before use. QX-314 chloride (abcam) was prepared in 100 mM stock solution in deionized distilled water and aliquots were kept at –20°C before use.

### Viral constructs and transduction

Adeno associated virus serotype 9 (AAV9) was used for expression of hM3Dq-mCherry cDNA in Cre-expressing animals. AAV9-hSYN-DIO-hM3D(Gq)-mCherry (titer: 2-5E13 GC/mL) was produced by the Canadian Neurophotonics Platform, Quebec, Canada. Newly born pups (postnatal day 0-2) were anesthetized on ice and administered intra-peritoneally by 10 µL of the viral construct using a Hamilton syringe connected to a 30G syringe tip (Becton Dickinson) through a Polyethylene tube (PE-10/10, Warner Instruments). Pups were returned to their parent cages and weaned after 21-28 days.

### Headpost implants

Poly(lactic acid) (PLA) was used for 3D printing of headposts (1h x 7d in mm at the base, 7h x 6d in mm at the shaft, and 3h x 13d in mm at the top). Adult male mice were anesthetized by isoflurane and stabilized on a warming pad after shaving the hair on the top of their head and application of lubricant eye ointment (Alcon). After application of disinfecting agent (chlorhexidine 2%) a 1.5-2 cm incision was made in the midline over the skull. After cleansing the surface of the skull, the headpost was placed on the skull in between the ears and was secured using dental cement (LangDental). For reinforcing the headpost placement for longitudinal studies, a bone anchor screw (Stoelting) was put in the bone surface beside the headpost shaft before applying the dental cement. After the cement cured, the skin was sutured around the base of the headpost and local anesthetic cream was applied (emla: Lidocaine 2.5% & Prilocaine 2.5%) before the animals were left to wake up. All animals received pre (right before surgery) and post (for 4 days) surgical analgesics (20 mg/kg/day Carprofen s.c. for 3 days) and were monitored for wound healing and proper hydration. Once the animals recovered from this procedure they would undergo a light anesthesia during which a cut pipet tip was glued to the top of the headpost to make an optic fiber holder keeping the light localized to the cheek. Animals were given at least two weeks of recovery before behavioral tests.

### Laser sources and light guides

A 473 nm diode-pumped solid-state (DPSS) laser (max 120 mW, LaserGlow) was used for selective activation of ChR2 while a 589 nm DPSS laser (max 100 mW, Changchun Dragon Lasers) was used as a yellow light source for control experiments. Light was guided through a 1 mm-diameter optical fiber (NA = 0.5) for skin (transdermal) stimulations and through a 0.2 mm-diameter optical fiber (NA = 0.37) for *in vitro* tests. For transdermal stimulations, unless otherwise stated, the lasers were set to 3.5-4.5 mW (constant power output) at the tip of the optical fiber and the tip was placed 2-5 mm away from the skin. A TTL pulse train generator (Prizmatix) was used for driving the lasers with 20 ms short pulses. For screening purposes, 3 s trains of 0.5-10 Hz pulses (20-500 ms on-time) with 0.01-90 mW powers were used in random orders to avoid desensitization due to prior exposures.

### Behavioral assays

For all behavioral studies, adult male mice were first familiarized with the experimenter, handling and injection types, and the environment of the experiment for at least one week, daily. Tests were done during the light cycle between 10am and 4pm. When needed, animals were shaved using a small electric shaver 2 days prior to the recording. All chemical interventions were followed by multi-angle video recordings for offline behavioral analysis. Video scorings were performed by trained experimenters blind to treatments. To further decrease possible bias within each experiment, long recordings were randomly cut into 8-15 minute clips, shuffled and mixed and put together after evaluations. Videos were scored manually using an in-house time stamping software which allowed precise recording of several behavioral responses and their duration within each clip.

For the cheek model of itch/pain discrimination, each scratching bout was defined as rapid brushing of the face by the hindpaw on the ipsilateral side. Each episode starts from the time scratching begins and ends with the hindpaw back on the ground or in the mouth. Pain behavior was defined as unilateral wiping of the ipsilateral side of the face by the forepaw. This behavior was distinct from grooming, defined as bilateral wiping of the face or any other actions on nonspecific sites of the body, e.g., rapid licking and biting of the chest, limbs and side areas. Contralateral scratching and wipings were not included in the behavioral analysis. For the nape of the neck model of itch quantification, scratching bouts were defined as rapid scuffing of the back area with either hindpaw.

For laser-evoked behaviors on the nape of the neck, scratching was defined similarly to the scratching behavior observed after chemical interventions: rapid treatment of the illuminated area by the hind paw. All other behavioral responses elicited by blue light were categorized as aversive: rapid avoidance, aggressive biting approaches toward the fiber optic, running and vocalization. It is noteworthy that wiping was not observed in these experiments as the nape is physically inaccessible by the forepaws of the animal. All animals received the different frequency-intensity protocols. No consistent relationship between illumination protocols and the evoked behavioral responses was observed.

For cheek illumination experiments, animals were acclimated to the observation chamber and the fiber optic attachment for at least one week. For each session of cheek illumination experiment, animals were brought to the testing chamber to acclimate for at least 30 min. In each session 8-10 trials of laser illumination protocols (i.e., different frequency, pulse duration, and intensity) were randomly applied for 3-5 s. At least 3 minutes of separation was allowed between trials and sessions were separated by at least 2 days for each animal. Although responses were more likely to be observed at the beginning of each session, no significant relationship was deduced between the illumination protocols and the probability of behavior induction.

For hindpaw illumination studies, animals were acclimated to the behavior observation chambers (10w x 5d x 8h cm) placed on a wire mesh for at least one hour in presence of the experimenter and the laser devices. Laser illumination pulses of 3 s were delivered to the plantar site of the hindpaws allowing at least 3 minutes in between stimulations on one paw.

For purinergic pain studies, animals were acclimated on the recording platform for at least 30 minutes. QX-314 conditioning injection in the plantar surface of the right hindpaw were made in 10  $\mu$ L volumes and the animals were returned to their recording chambers. 30 minutes after the conditioning injection 10  $\mu$ L of 20 mM  $\alpha\beta$ meATP was injected intraplantary in the same paw and the animals were recorded for 5 minutes. Close observation of the animals from 3 different angles was performed in slow-motion by blind experimenters to detect exact start and end points of lifting or licking of the right hindpaw.

### In vitro preparations and assays

For calcium imaging, cultured primary DRG and TG sensory neurons were loaded for 45 minutes in 2 mM Fura2-acetoxymethyl ester. Cells were then washed and kept for an additional 45 minutes in extracellular medium with no Fura-2 (37°C, 5% CO<sub>2</sub>) for desesterification. Loaded cells were imaged every 2 s with 340 nm and 380 nm excitation filters using a Nikon (Eclipse TE300) wide-field microscope and Metafluor software (Molecular Devices). Background corrected normalized ratios of emission under 340 nm excitation divided by emission under 380 nm excitation are reported as proxies of relative intracellular calcium levels. Cultures were under constant perfusion of external solution (pH 7.4) consisting of 152 mM NaCl, 5 mM KCl, 2 mM CaCl<sub>2</sub>, 1 mM MgCl<sub>2</sub>, 10 mM HEPES, and 10 mM glucose with or without test drugs. Response criteria was defined as drug-induced  $\Delta$ ratios 5 times larger than baseline fluctuations. All responsive cell traces were manually verified after experiments.

For electrophysiology studies on neuronal excitability and controllability by blue light, cultured primary sensory neurons were patched onto with glass pipets (5-9 M $\Omega$ ) in whole cell configuration and perfused with artificial cerebrospinal fluid (pH 7.4) containing 152 mM NaCl, 5 mM KCl, 2 mM CaCl<sub>2</sub>, 1 mM MgCl<sub>2</sub>, 10 mM HEPES, and 10 mM glucose. Recording patch pipets were filled with internal solution (pH 7.2) containing 130 mM K-gluconate, 1 mM MgCl<sub>2</sub>, 10 mM HEPES, 5 mM EGTA, 3 mM MgATP, and 0.4 mM GTP. Responses to blue light delivered by optic fiber were measured in voltage and current clamp modes in pClamp 9 on an amplifier Axopatch 200B connected to a digitizer Digidata 1320A (Molecular Devices).

### Ex vivo tissue preparations and morphology

For expression and histological validations, animals were perfused by intracardiac perfusion of 10 mL phosphate buffer saline followed by 30 mL 4% formaldehyde solution (pH 7.4) after deep isoflurane anesthesia. DRGs, TGs, spinal cords and skin samples were collected and post-fixed for 2-4 hours in formaldehyde solution before they were transferred to a 30% sucrose solution for minimum 48 hours. Sections were cut embedded and frozen in optimal cutting temperature (OCT) solution on a Leica cryostat (DRG and

TG: 14  $\mu\text{m}$ ; skin and spinal cord: 30  $\mu\text{m}$ ). Skin and ganglia sections were mounted directly on microscope slides while spinal cord sections were transferred to 24-well plates for staining procedures.

For immunohistochemistry, free-floating or mounted sections were washed three times for 10 minutes each with phosphate buffered saline containing 0.2% Triton X-100 (PBST) before blocking with 10% normal serum (goat or donkey). Sections were left in 5% normal serum containing primary antibodies (dilution 1:2000) on a shaker in a cold room (4°C) overnight. Rabbit anti-PGP9.5 (Ultraclone RA95101) as a marker for overall skin innervation and monoclonal rat anti-mCherry (Thermo Fisher Scientific M11217) were used as primary antibodies. After 3 washes with PBST, secondary antibodies (1:500) was added to the sections for 2 hours at room temperature. Donkey anti-rat conjugated to Cy-5 (Jackson Immunoresearch) and goat anti-rabbit conjugated to Alexa 568 (Life Technologies) were used as secondary antibodies. Finally, the sections were mounted and imaged with Zeiss LSM710 or Leica SP8 confocal microscopes.

### QUANTIFICATION AND STATISTICAL ANALYSIS

All statistical tests were performed using MATLAB and figures were generated using the Seaborn data visualization package in Python. Individual tests (unpaired and paired t tests, one-way and two-way ANOVA), their respective post hoc tests (Bonferroni post-test) and n (sampling size) are mentioned in the results section and the figure legends. Errors are presented as standard error of mean (SEM) and significance levels are indicated in each comparison:  $p < 0.05$  (\*),  $p < 0.01$  (\*\*) and  $p < 0.001$  (\*\*\*)